Nitric Oxide Dissociates Lipid Oxidation from Apoptosis and Phosphatidylserine Externalization during Oxidative Stress†

James P. Fabisiak,*,‡ Vladimir A. Tyurin,‡,§ Yulia Y. Tyurina,‡,§ Andrey Sedlov,‡ John S. Lazo,|| and Valerian E. Kagan‡,||

Department of Environmental and Occupational Health, School of Public Health, RIDC Park, 260 Kappa Drive, University of Pittsburgh, Pittsburgh, Pennsylvania 15238, and Department of Pharmacology, School of Medicine, University of Pittsburgh, Pittsburgh, Pennsylvania 15261

Received June 2, 1999; Revised Manuscript Received October 21, 1999

ABSTRACT: Oxidative stress in biological membranes can regulate various aspects of apoptosis, including phosphatidylserine (PS) externalization. It is not known, however, if the targets for these effects are lipids or proteins. Nitric oxide (NO), a bifunctional modulator of apoptosis, has both antioxidant and prooxidant potential. We report here that the NO donor PAPANONOate completely protected all phospholipids, including PS, from oxidation in HL-60 cells treated with 2,2′-azobis(2,4-dimethylisovaleronitrile) (AMVN), presumably via the ability of NO to react with lipid-derived peroxyl radicals and terminate the propagation of lipid peroxidation. PAPANONOate, however, had no effect on PS externalization or other markers of apoptosis following AMVN. Therefore, PS oxidation is not required for PS externalization during AMVN-induced apoptosis. PS externalization was accompanied by inhibition of aminophospholipid translocase (APT). NO potentiated AMVN inhibition of APT. Treatment with PAPANONOate alone produced modest (20%) inhibition of APT without PS externalization. NO did not reverse AMVN-induced oxidation of glutathione and protein thiols. We speculate that APT was sensitive to AMVN and/or NO via modification of protein thiols critical for functional activity. Therefore, the lipoprotective effects of NO were insufficient to prevent PS externalization and apoptosis following oxidative stress. Other targets such as protein thiols may be important redox-sensitive regulators of apoptosis initiation and execution. Thus, in the absence of significant peroxynitrite formation, NO's antioxidant effects are restricted to protection of lipids, while modification of protein substrates continues to occur.

We have previously shown that apoptosis following oxidative stress is associated with the selective oxidation of the aminophospholipid phosphatidylserine (PS)[1] (*1, 2*). The potential importance of this observation is underscored by the fact that specific relocation of PS from the internal surface to the external surface of the plasma membrane is fundamental for the recognition and elimination of apoptotic cells by phagocytic macrophages (*3*). PS externalization presumably arises, in part, through inactivation of aminophospholipid translocase (APT), whose normal surveillance function maintains the strict asymmetric distribution of PS in normal cells (*4*, *5*). Thus, specific oxidative events occurring within the hydrophobic core of biomembranes could have important signaling functions during apoptosis, especially for modulating PS translocation.

Nitric oxide (NO) is a pluripotent regulator of diverse cellular functions (*6*). By virtue of its free radical nature, it is capable of participating in a variety of redox reactions that can lead to its reversible and irreversible reactions with a variety of target molecules within cells (*7*). Its chemical reactivity and abundance during inflammation ensure that NO will play an important position in the regulation of tissue injury, especially that resulting during oxidative stress. The precise role, however, remains controversial since NO can both augment and prevent tissue and cellular damage. Under certain conditions, NO can act to promote nitrosation of thiol-containing proteins (*8*−*11*). In addition, NO can react with superoxide to produce the powerful oxidant peroxynitrite (*12*), and readily oxidize protein and nonprotein sulfhydryls (*13*), as well as membrane lipids (*14*). Several studies indicate the potential of NO to enhance cellular injury (*15*, *16*).

† This work was supported by NIH Grants ES-09387 (J.P.F.) and CA-43917 (J.S.L.), AICR Grant 97B128 (V.E.K.), Johns Hopkins Center for Alternatives to Animal Testing Grant 9829 (V.E.K.), the NCI Oncology Research Faculty Development Program (V.A.T.), and International Neurological Science Fellowship Program F05NS10669 by NIH/NINDS and WHO (Y.Y.T.).

* To whom correspondence should be addressed at the Department of Environmental and Occupational Health, School of Public Health, RIDC Park, 260 Kappa Dr., University of Pittsburgh, Pittsburgh, PA 15238. Phone: (412) 967-6523. FAX: (412) 624-1020. E-mail: fabs+@pitt.edu.

‡ Department of Environmental and Occupational Health, School of Public Health.

§ On leave from the Institute of Evolutionary Physiology and Biochemistry, Russian Academy of Science, St. Petersburg, Russia, 194223.

|| Department of Pharmacology, School of Medicine.

[1] Abbreviations: AMVN, 2,2′-azobis(2,4-dimethylisovaleronitrile); APT, aminophospholipid translocase; *cis*-PnA, *cis*-parinaric acid; DAF-2DA, 4,5-diaminofluorescein diacetate; GSH, reduced glutathinone; NO, nitric oxide; PAPANONOate, (*Z*)-[*N*-(3-ammoniopropyl)-*N*-(*n*-propyl)-amino]-diazen-1-ium-1,2-diolate; PC, phosphatidylcholine; PEA, phosphatidylethanolamine; PI, phosphatidylinositol; PS, phosphatidylserine; HP-TLC, high-performance thin-layer chromatography; HPLC, high-pressure liquid chromatography.

10.1021/bi9912544 CCC: $19.00
Published on Web 12/08/1999

In contrast, NO can also serve a protective function during oxidative stress. By virtue of its electron-donating ability, NO can serve to diminish oxidative stress by quenching lipid peroxyl and other radical species (*17, 18*). NO-induced protection from oxidant-mediated cell and tissue injury has been observed (*19, 20*). While some studies have noted the potential for NO to induce apoptosis (*21, 22*), several others have observed that NO can inhibit this mode of cell death (*23, 24*). More recently, the survival enhancing function of NO has been shown, in part, to include the direct inactivation of caspase proteases required for apoptosis (*25, 26*).

Given the dichotomous role of NO as both a cytotoxic and a cytoprotective mediator, we decided to investigate the ability of NO to modulate oxidation of sensitive biomolecules as well as PS externalization and apoptosis in HL-60 cells following exposure to a lipophilic azo-initiator of peroxyl radicals, 2,2′-azobis(2,4-dimethylisovaleronitrile) (AMVN). Our results indicate that although NO can act as a potent and efficacious inhibitor of oxidation of all membrane phospholipids, including PS, this activity is insufficient to prevent PS externalization and apoptosis following AMVN.

MATERIALS AND METHODS

Materials. All tissue culture media and additives were obtained from GIBCO BRL (Gaithersburg, MD) except fetal bovine serum (FBS), which was from HyClone (Logan, UT). Proteinase K, ribonuclease (RNase) T1, and RNase A were from Boehringer-Mannheim (Indianapolis, IN). *cis*-Parinaric (*cis*-PnA) [(9*Z*,11*E*,13*E*,15*Z*)-octadecatetraenoic acid] was obtained from Molecular Probes (Eugene, OR). 1-Palmitoyl-2-[6-[(7-nitro-2,1,3-benzoxadiazol-4-yl)amino]caproyl]-*sn*-glycero-3-phosphoserine (NBD-PS) and 1-palmitoyl-2-[6-[(7-nitro-2,1,3-benzoxadiazol-4-yl)amino]caproyl]-*sn*-glycero-3-phosphocholine (NBD-PC) were from Avanti Polar Lipids (Alabaster, AL). HPLC-grade solvents were from Fisher Scientific (Pittsburgh, PA). 2,2′-Azobis(2,4-dimethylisovaleronitrile) (AMVN) was supplied by Wako Chemicals (Richmond, VA), and (*Z*)-[*N*-(3-ammoniopropyl)-*N*-(*n*-propyl)amino]-diazen-1-ium-1,2-diolate (PAPANONOate, NOC-15) was from either Alexis Corp. (San Diego, CA) or Cayman Chemical, Co. (Ann Arbor, MI). 4,5-Diaminofluorescein diacetate (DAF-2A) was obtained from Calbiochem (La Jolla, CA). The maleimide-based thiol reagent ThioGlo-1 was obtained from Covalent Associates, Inc. (Woburn, MA). All other chemicals and reagents were molecular biology grade.

Cell Culture and Treatments. Stock HL-60 cells were routinely split at 3−4 day intervals and cultured in RPMI 1640 containing 15% FBS and supplemented with penicillin (100 units/mL), streptomycin (100 μg/mL), glutamine (2 mM), and Fungizone (1.25 μg/mL). For experiments, cells obtained from stock cultures were counted, centrifuged, and resuspended in the indicated media at a density of 1×10^6 cells/mL. PAPANONOate stock solutions (10 mM) were freshly prepared at each use in 20 mM NaOH. AMVN was applied at the indicated concentrations from a 100 mM stock solution prepared in DMSO. To assess the protective effects of the NO donor, we applied PAPANONOate to cells 15 min prior to the addition of AMVN. Control cells received equivalent concentrations of the vehicles alone. Incubations were carried out at 37 °C for the times indicated and then processed for assays of lipid and thiol oxidation, as well as apoptosis.

Quantification of NO-release during treatment of cells with PAPANONOate was assessed using the NO-specific cell-permeable fluoroscent probe DAF-2DA. Cells were preloaded by incubation in serum-free RPMI containing 10 μM DAF-2DA for 1 h at 37 °C. Cells were then washed twice and treated for various times as described above. Aliquots of cells were then taken and diluted 10-fold in L1210 buffer, and fluorescence was recorded with excitation at 495 nm and emission at 515 nm using a Shimadzu spectrofluorometer RF-5301PC.

Lipid Peroxidation. Lipid peroxidation in individual phospholipid classes was performed using the fluorescent oxidation-sensitive fatty acid *cis*-PnA essentially as previously described by our laboratory (*1, 2*). We have developed this assay as a sensitive method to measure lipid peroxidation in live cells independent of phospholipid repair reactions (*27*). HL-60 cells were allowed to metabolically incorporate *cis*-PnA into phospholipids by incubation with *cis*-PnA/human serum albumin complex (2 μg/mL, final *cis*-PnA concentration) in L1210 buffer (115 mM NaCl, 5 mM KCl, 1 mM $MgCl_2$, 5 mM NaH_2PO_4, 10 mM glucose, and 25 mM HEPES, pH 7.4) at a density of 1×10^6 cells/mL for 2 h at 37 °C. Free *cis*-PnA was removed by vigorous washing in the presence of human serum albumin, and cells were finally resuspended in serum-free L1210 buffer (1×10^6 cells/mL). Cells were treated with AMVN and/or PAPANONOate for 2 h at 37 °C. Following treatment, cells were recovered by centrifugation and lysed in 0.5 mL of ice-cold methanol containing butylated hydroxytoluene (0.1 mg), and phospholipids were extracted by the Folch procedure (*28*). Individual phospholipids were then resolved, and the fluorescent content of each species was determined by high-performance liquid chromatography (HPLC) as previously described (*1, 2, 27*). The amount of *cis*-PnA fluorescence in each phospholipid was normalized to the amount of total inorganic phosphate in the total lipid extract determined by the method of Chalvardijan and Rubnicki (*29*). The effect of various experimental treatments on the phospholipid composition of HL-60 cells was assessed using two-dimensional HP-TLC as previously described (*2*).

Thiol Oxidation. HL-60 cells (1×10^6 cells/mL) were incubated in the presence or in the absence of AMVN (500 μM) and PAPANONOate (10 μM) at 37 °C for 2 h in L1210 buffer (pH 7.4). Cells were collected by centrifugation and lysed by sequential freezing at −80 °C and thawing at room temperature. The disrupted cell pellet was resuspended in a volume of L1210 buffer (pH 7.4) corresponding to 2×10^6 cells/mL. Aliquots of crude cell homogenate (4×10^5 cells) were taken for thiol determination in the total homogenate. The cell homogenate was then centrifuged at 10000*g* for 20 min, and the supernatant was decanted. Aliquots of supernatant were used for determination of soluble glutathione (GSH) and protein thiols as described below.

ThioGlo-1, a maleimide reagent producing a highly fluorescent product upon reaction with SH groups (*30*), was used to determine the total protein sulfhydryl and GSH content in homogenates as previously descibed by us (*31*). GSH content was estimated by an immediate fluorescence response registered upon addition of ThioGlo-1 (20 μM, final concentration) to the cell homogenate. Once the initial

response had reached a plateau, total protein thiols were determined as an additional response observed after the addition of SDS (2 mM, final concentration) to the same sample. The identities of these two thiol pools as GSH and protein SH groups, respectively, were confirmed in experiments where pretreatment of cell homogenates with glutathione peroxidase completely abrogated the initial fluorescence response with no change in the response following addition of SDS. Fluorescence was measured with a Shimadzu spectrofluorometer RF-5301PC using excitation and emission wavelengths of 388 and 500 nm, respectively. Data were analyzed using RF-5301PC Personal Fluorescence Software (Shimadzu). Actual thiol content was determined with a standard curve constructed using pure GSH (0.2−6 μM) in phosphate buffer (pH 7.4).

To determine the electrophoretic pattern of protein thiols, HL-60 cells were treated with 500 μM AMVN and various concentrations of PAPANONOate for 2 h at 37 °C in serum-free RPMI. Following incubation, 20×10^6 cells were collected by centrifugation, washed, and resuspended in 1 mL of 50 mM phosphate buffer (pH 7.4) containing PMSF (100 μg/mL), antipain (2 μg/mL), pepstatin (1 μg/mL), and leupeptin (1 μg/mL). Cells were sonicated for three 5 s bursts on ice with a 4710 series Ultrasonic Homogenizer (Cole-Palmer Instruments, Chicago, IL). A 250 μL aliquot of homogenate was filtered through a Microcon YM-3 (3000 MW cutoff) (Millipore) centrifugal filter in order to remove GSH. Final retentate (30−40 μL) was diluted up to the initial volume and filtration continued for another 30 min. After this procedure, the GSH content was no higher than 1.5 μM. Protein concentration was measured by Bradford assay (Bio-Rad) and adjusted to 1 mg/mL. Twenty microliter aliquots of protein sample were added to 180 μL of 50 mM phosphate buffer, 30 mM SDS, and 10 μM ThioGlo 1. The mixture was incubated at 60 °C for 40 min then left at room temperature for 20 min.

Samples containing 2 μg of protein were loaded onto 1.5 mm thick 8% acrylamide gels, and electrophoresis was carried out under standard conditions with the exception that the loading buffer did not contain bromophenol blue and samples were applied to the gel without additional heating. ThioGlo-1 fluorescence derivatized to protein thiols was then visualized with a Bio-Rad Fluor-S Multiimager equipped with a UV light source (290−365 nm) and built-in CCD camera with the emission filter at 530 nm (broad range). Image capture and subsequent analysis were performed using Bio-Rad Multi-Analyst Software.

Apoptosis. Nuclear morphology was assessed as previously described using Hoescht 33342 fluorescent staining (*1*, *2*). The percentage of apoptotic cells was determined by counting the number of nuclei showing chromatin condensation and fragmentation characteristic of apoptosis after observing at least 300 total cells. Low molecular weight DNA fragmentation was determined using conventional gel electrophoresis as described previously (*1*, *2*). Briefly, aliquots of 1×10^6 cells were collected after treatment by centrifugation at 400g for 10 min. Washed cell pellets were lysed and digested overnight at 50 °C with proteinase K (1 mg/mL, final concentration). Samples were incubated with 10 μg of RNase A and 200 units of RNase T1 at 37 °C for 1 h. Samples were electrophoresed in 2% agarose gels (60 V) for approximately 4 h. Gels were stained with ethidium bromide (1 μg/mL) and evaluated under UV illumination.

Annexin V Binding. Annexin V binding to cells was performed using flow cytometry essentially as previously described (*1*, *2*) with a commercially available staining kit (R & D Systems, Minneapolis, MN). Briefly, HL-60 cells were placed in serum-free RPMI 1640 (1×10^6 cells/mL) and then treated with or without AMVN. Cells (7.5×10^5) were recovered at the indicated times and washed twice in ice-cold PBS. Cells were incubated with annexin V−fluorescein conjugate (1 μg/mL, final concentration) and propidium iodide (5 μg/mL) for 20 min at room temperature. Cells were analyzed with a FACScan flow cytometer (Becton-Dickenson) with simultaneous monitoring of green fluorescence (530 nm, 30 nm band-pass filter) for annexin V−fluorescein and red fluorescence (long-pass emission filter that transmits light >650 nm) associated with propidium iodide.

Fluorescamine Labeling of Externalized Aminophospholipids. Labeling of externalized aminophospholipids, PS and PEA, with fluorescamine was carried out essentially as previously described by our laboratory (*2*). Briefly, after treatments, HL-60 cells (4×10^7) were suspended in labeling buffer [150 mM NaCl, 5 mM KCl, 1 mM $MgCl_2$, 2 mM $CaCl_2$, 5 mM $NaHCO_3$, 5 mM glucose, and 20 mM HEPES (pH 8.0)]. Fluorescamine was added (200 μM, final concentration), and cells were gently agitated for 15 s. Three milliliters of 40 mM Tris-HCl (pH 7.4) was then added. Cells were recovered by centrifugation and then extracted. Lipids were applied to HP-TLC plates and developed in the first dimension using chloroform/methanol/28% ammonium hydroxide (65:35:5, v/v/v) followed by chloroform/acetone/methanol/glacial acetic acid/water (50:20:10:10:5). Individual spots corresponding to fluorescamine-modified PS and PEA (mPS and mPEA) were localized by exposure to fluorescent light. Unmodified phospholipids were visualized following exposure to iodine vapor. The identity of specific phospholipid species was verified using purified standards. The phosphorus content of PS and PEA (and fluorescamine-modified mPS and mPEA) was determined according to Bottcher et al. (*32*) after scraping representative spots from the plate. The amount of modified mPS and mPEA was expressed as a percentage of the total PS and PEA (unmodified plus modified) recovered from the plate based on phosphorus assay.

Caspase Activity. Caspase-3 activity in cell lysates was measured using a fluorometric assay kit from Kamiya Biomedical Co. (Seattle, WA) according to the manufacturer's instructions, except that duplicate samples were prepared for measurement in 2× reaction buffer with and without DTT (5 mM, final concentration). Briefly, 1×10^6 cells were collected and lysed in 50 μL of ice-cold Lysis Buffer supplied with the kit. 2× Reaction Buffer (50 μL) with or without 10 mM DTT was added to each lysate and kept on ice. Five microliters of 1 mM fluorescent substrate, DVED−7-amino-4-trifluoromethylcoumarin conjugate, was added and reaction started by transferring samples to individual wells of a 96-well microtiter plate (Corning). Free 7-amino-4-trifluoromethylcoumarin fluorescence was determined at zero time and following 1 h incubation at 37 °C using a CytoFlour 2350 (Millipore) fluorescence plate reader using excitation filter 360/40 and emission filter 530/25. The

specific activity for caspase-3 was determined by parallel incubations in the presence of the inhibitor DEVD-CHO (10 μM, final concentration). Caspase-3 activity was expressed as the amount of DEVD-CHO-inhibitable product produced within 1 h and determined from a standard curve prepared using purified 7-amino-4-trifluoromethylcoumarin.

Aminophospholipid Translocase Activity. Aminophospholipid translocase (APT) activity was measured using modifications of the methods of McIntyre and Sleight (*33*) and Williamson et al. (*34*). HL-60 cells were obtained from stock cultures or treated with AMVN and/or PAPANONOate in L1210 buffer as described for lipid peroxidation experiments. Cells (approximately 4×10^6) were centrifuged (400*g*, 10 min) and washed once in incubation buffer (136 mM NaCl, 2.7 mM KCl, 2 mM $MgCl_2$, 5 mM glucose, 10 mM HEPES, pH 7.5). The cell pellet was resuspended in incubation buffer (1 mL/5×10^6 cells) containing 500 μM phenylmethylsulfonyl fluoride (PMSF), transferred to a microfuge tube, and placed in ice−water for 10 min. NBD-labeled phospholipids were prepared by removing 30 μL of stock in chloroform (1 mg/mL) using a metal/glass syringe and evaporating to dryness in a glass tube with nitrogen. NBD-labeled phospholipids were then dissolved in 19 μL of EtOH with vigorous mixing and sonication. NBD-phospholipids were then added to cells (final concentration, 10 μM) and incubated for 10 min at 4 °C. Labeled cells were centrifuged and resuspended at the same density in incubation buffer with PMSF. The cell suspension was then placed in a 28 °C water bath to initiate internalization, and 50 μL aliquots of cell suspension were removed at various times and placed into 950 μL of incubation buffer including the reducing agent sodium dithionite (10 mM). Fluorescence (excitation = 470 nm, emission = 540 nm) was recorded between 30 s and 1 min later. The fluorometer was calibrated to zero using unlabeled cells, and time zero internalized fluorescence (FL_0) was obtained using ice-cold cells placed directly in reducing incubation buffer. Samples from the last time point were also placed in incubation buffer without dithionite to obtain a measure of the total available fluorescence (FL_{total}). The internalized fluorescence at various times (FL_t) was then normalized as a percent of the total available by the following equation:

$$\% \text{ internalized} = (FL_t - FL_0)/(FL_{total} - FL_0) \times 100$$

To test the effect of sodium vanadate on internalization, the inhibitor was present during the preincubation at 4 °C, as well as during the internalization process conducted over 15 min.

RESULTS

Effects of NO on AMVN-Induced Phospholipid Oxidation. By virtue of its lipophilic nature, AMVN-induced oxidative stress is considered to occur primarily within the environment of cellular membranes (*35*). Phospholipids, therefore, are considered primary targets for oxidative attack. Figure 1 shows the ability of AMVN to induce widespread oxidation of *cis*-PnA that has been incorporated into multiple phospholipid species including PC, PEA, PI, and PS. In the absence of the NO donor, PAPANONOate, 2 h treatment of cells with AMVN (500 μM) oxidized 86.2% of *cis*-PnA incorporated into PC, 87.5% in PEA, 88.9% in PI, and 73.1% in PS. It is important to point out that *cis*-PnA-labeled phospholipids represent only a small pool of total phospholipids (<8%) in HL-60 cells. Thus, the oxidation measured here actually reflects relatively low levels of overall oxidation and thus provides a highly sensitive, minimally invasive, measure of lipid peroxidation in live cells under conditions when the bulk of cellular lipids are spared oxidative attack.

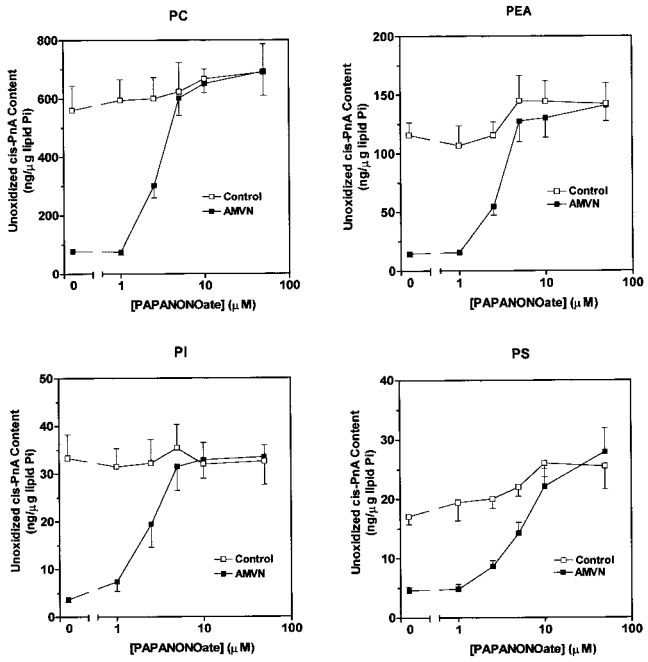

FIGURE 1: NO inhibits AMVN-induced oxidation of all major phospholipids in HL-60 cells. HL-60 cells were metabolically labeled with *cis*-PnA as described under Materials and Methods. Cells were then preincubated with various concentrations of the NO donor, PAPANONOate, for 15 min followed by exposure to 500 μM AMVN for 2 h. Control cells were exposed to PAPANONOate alone and incubated in the absence of AMVN. Phospholipids were then extracted and subjected to HPLC for quantification of the amount of unoxidized fluorescent *cis*-PnA in various phospholipids including phosphatidylcholine (PC), phosphatidylethanolamine (PEA), phosphatidylinositol (PI), and phosphatidylserine (PS). Data are expressed as μg of *cis*-PnA/μg of total lipid phosphorus (mean ± SD determined from 4 observations).

Table 1 shows that the phospholipid composition of HL-60 cells after incubation in the presence of AMVN and/or PAPANONOate is identical to that observed in control untreated cells. Most importantly, this indicates that despite oxidation of almost 90% of the *cis*-PnA contained in phospholipids, the bulk of the phospholipids were recovered in their native form. No smearing of spots indicative of phospholipid oxidation products was observed after HP-TLC. This would indicate the level of oxidation produced here did not overwhelm the capacity of HL-60 cells to repair oxidized phospholipids by deacylation/reacylation mechanisms. The small increase in lyso-PC observed here after AMVN suggests the operation of these repair pathways.

Inclusion of PAPANONOate during incubation provided a concentration-dependent protection to all phospholipids. Protection occurred only after 1 μM PAPANONOate and was essentially complete at 5 μM for PC, PEA, and PI. PS appeared somewhat more resistant since complete protection was not achieved until 10 μM or higher concentrations of the NO donor. Exposure of cells to PAPANONOate alone did not induce lipid oxidation, and, in fact, showed a trend

Table 1: Effect of AMVN and PAPANONOate on Phospholipid Composition of HL-60 Cells[a]

phospholipid	control	PAPANONOate	AMVN	AMVN + PAPANONOate
phosphatidylcholine	49.6 ± 2.5	50.3 ± 3.3	50.0 ± 2.8	49.2 ± 3.3
phosphatidylethanolamine	28.9 ± 1.6	28.7 ± 2.5	28.2 ± 1.9	29.5 ± 2.9
phosphatidylserine	6.3 ± 1.2	6.8 ± 1.0	5.8 ± 1.1	6.5 ± 1.0
phosphatidylinositol	6.4 ± 1.1	5.4 ± 1.0	6.1 ± 0.9	5.7 ± 0.9
sphingomyelin	6.2 ± 0.8	5.8 ± 0.9	6.2 ± 1.0	6.0 ± 1.1
diphosphatidylglycerol	2.0 ± 0.9	2.1 ± 0.9	2.4 ± 0.8	2.0 ± 0.8
lysophosphatidylcholine	0.6 ± 0.2	0.9 ± 0.3	1.3 ± 0.3	1.1 ± 0.3

[a] Data are expressed as mean ± SEM percent of total phospholipids ($n = 4$).

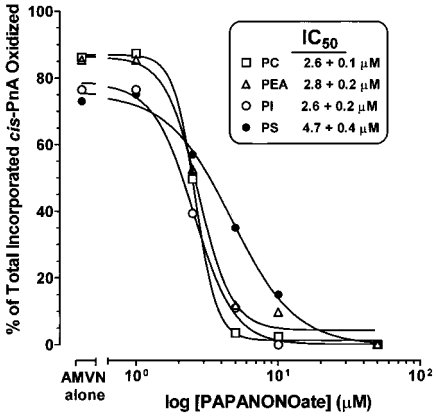

FIGURE 2: Concentration−response curves for PAPANONOate inhibition of AMVN-induced oxidation in various phospholipid classes. The amount of *cis*-PnA oxidized in PC, PEA, PI, and PS was determined at various concentrations of PAPANONOate and expressed as a percent of total incorporated *cis*-PnA. Data were curve-fitted, and IC_{50} was determined with GraphPad Prism software using a sigmoidal dose−response with varying slope model.

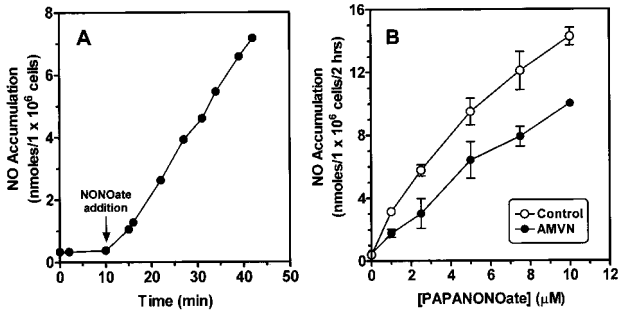

FIGURE 3: Quantification of NO release from PAPANONOate in intact cells and NO consumption by AMVN-dependent processes. HL-60 cells were placed in serum-free RPMI 1640 and incubated with 10 μM DAF-2DA for 1 h at 37 °C. Cells were then washed twice, and the final pellet was resuspended in L1210 medium with or without AMVN and placed at 37 °C. Aliquots were taken at the indicated times and diluted 10-fold in L1210 buffer, and fluorescence was recorded (excitation = 495 nm, emission = 515 nm). Panel A shows the increase in NO-dependent DFA-2DA fluorescence that occurs immediately after the addition of the 10 μM NO donor PAPANONOate. Data represent a single experiment that was repeated once with identical results. Panel B depicts the 2 h cumulative NO-mediated DFA-2DA fluorescence produced by various concentrations of PAPANONOate in HL-60 cells in the absence and presence of AMVN. Cells were preincubated with PAPANONOate for 15 min prior to the addition of AMVN. Data represent mean ± SD of triplicate observations per point. When not visible, the SD is within the size of the symbol.

for the inhibition of the small spontaneous oxidation observed over the 2 h incubation. Figure 2 shows the concentration−response curves for PAPANONOate-induced inhibition of phospholipid oxidation in each of these four phospholipids. Note that calculation of IC_{50} revealed very similar potencies for PAPANONOate protection of PC, PI, and PEA (2.6−2.8 μM). In contrast, IC_{50} for inhibition of PS oxidation was higher than that observed for the other phospholipids. In addition, the slope of the inhibition curve for PS was less steep than that observed for other phospholipids. Since 10 μM PAPANONOate appeared sufficient to completely inhibit oxidation in these major phospholipid classes, this concentration was chosen for further study.

We employed the NO-specific fluorescent probe DAF-2DA to determine the amount of NO released during PAPANONOate treatment and whether AMVN-induced oxidative stress could diminish the steady-state concentration of free NO. HL-60 cells were first preloaded with DAF-2DA and then treated with 10 μM PAPANONOate. The time course of cellular NO-induced DAF-2DA fluorescence is shown in Figure 3A. DAF-2DA fluorescence remained unchanged during the 10 min preincubation prior to PAPANONOate addition. Fluorescence then rapidly increased in a time-dependent manner immediately upon addition of the NO donor, indicating that NO was indeed released at a linear rate over the period of incubation. The absolute amount of NO produced was calculated from a standard curve constructed from a series of PAPANONOate concentrations measured in phosphate buffer at times when release of NO was shown to be complete by a plateau in the fluorescent response.

If AMVN-derived radicals (either AMVN-derived peroxyl radicals themselves or other radical species initiated by AMVN-induced oxidative stress, i.e., lipid peroxyl or alkoxyl radicals) could directly interact with NO, then these species should compete with DAF-2DA for NO. Therefore, we hypothesized that the extent of cellular DAF-2DA fluorescence after addition of PAPANONOate would be reduced when cells were undergoing AMVN-induced oxidative stress. Figure 3B shows the DAF-2DA fluorescence measurement of NO produced by several concentrations of PAPANONOate in the presence and absence of AMVN (500 μM). The difference in measured NO between these two lines likely represents that amount of NO consumed by reaction with AMVN-dependent radicals. For example, the difference between control and AMVN-treated cells at 10 μM PAPANONOate revealed that approximately 4.25 nmol of NO/1 $\times$ 10^6 cells was consumed by these AMVN-dependent radical/NO interactions. No AMVN-dependent decrement in fluorescence was observed if the cell-impermeable, nonesterified congener of the NO probe, DAF-2, was used (data not shown), indicating that the AMVN-dependent consumption of NO occurred intracellularly. Furthermore, AMVN-derived radicals or lipid peroxidation products did not quench

Table 2: PAPANONOate Fails To Block Formation of Apoptotic Nuclei in HL-60 following AMVN[a]

treatment	% apoptotic nuclei, time after AMVN	
	2 h	5 h
RPMI + 10% FBS		
control	7.9 ± 2.8	9.3 ± 2.0
AMVN (500 μM)	21.9 ± 6.9[b]	37.2 ± 5.2[b]
AMVN + PAPANONOate (10 μM)	19.0 ± 6.6[b]	36.1 ± 6.8[b]
serum-free RPMI		
control	15.1 ± 7.8	21.6 ± 7.0
AMVN (500 μM)	46.2 ± 12.2[b]	69.1 ± 4.8[b]
AMVN + PAPANONOate (10 μM)	37.0 ± 17.0[b]	65.0 ± 6.1[b]

[a] Data represent mean ± SEM of 6 and 4 experiments for FBS and serum-free conditions, respectively. [b] Denote statistically significant difference from control by 1-way ANOVA and Newman−Keuls multiple comparison test.

the fluorescence yield of the preformed DAF-2/NO complex (data not shown).

AMVN, NO, and Apoptosis. (A) Nuclear Morphology. We next examined the ability of NO to modulate apoptosis following AMVN-induced oxidative stress. For these studies, we first compared the ability of AMVN to induce apoptosis under serum-replete and serum-deprived conditions. Apoptosis was first assessed using Hoescht 33342 nuclear staining and the acquisition of a characteristic nuclear morphology *(1, 2)*.

Table 2 shows the percentage of cells showing this apoptotic nuclear morphology visualized by Hoescht 33342 after exposure to 500 μM AMVN in the presence and absence of PAPANONOate. Incubations were first carried out in the presence of 10% FBS, where AMVN induced the apoptotic morphology in approximately 25% of cells by 2 h and nearly 40% by 5 h of exposure. Apoptosis in the absence of AMVN was less than 10% over this period of time. When PAPANONOate (10 μM) was included with AMVN, the extent of apoptosis remained unchanged compared to AMVN alone. The extent of apoptosis in the presence of PAPANONOate alone was the same as that observed in untreated control cells (data not shown).

To more closely mimic the serum-free conditions experienced during the lipid peroxidation assays and determine if failure of PAPANONOate to inhibit apoptosis was possibly due to quenching of NO generation or availability by serum proteins, we carried out similar experiments under serum-free conditions. In this case, the basal rate of apoptosis in untreated cells was slightly higher than in the presence of serum (15% at 2 h, 22% at 5 h). The response to AMVN alone was also greater than that observed in the presence of serum and reached approximately 70% of total cells after 5 h exposure. PAPANONOate again had essentially no effect on AMVN-induced apoptosis. Studies revealed that PAPANONOate alone did not produce any apoptosis above that observed under the untreated control incubations (data not shown).

Several further experiments were also conducted to verify the inability of PAPANONOate to inhibit AMVN-induced apoptosis despite its pronounced effect on lipid peroxidation. Since the release of NO from PAPANONOate is markedly pH-dependent, similar experiments were carried out in a CO_2-independent medium, Leibovitz's L-15 supplemented with glucose to match RPMI and adjusted to various pHs. Decomposition of the PAPANONOate at 37 °C for pHs 7.0, 7.4, and 7.8 revealed approximate half-lives for PAPANONOate of 10, 20, and 40 min, respectively. Analysis of apoptosis under these same incubation conditions, however, failed to uncover any significant effect of PAPANONOate on basal or AMVN-induced apoptosis (data not shown). Furthermore, increasing concentrations of PAPANONOate (up to 100 μM) were also without appreciable effect. Similarly, exposure of cells to lower concentrations to AMVN (100 μM) did not permit a protective effect of PAPANONOate to be observed. Thus, NO did not possess the ability to modulate AMVN-induced apoptosis despite its significant protective effect on oxidation of all major classes of phospholipids.

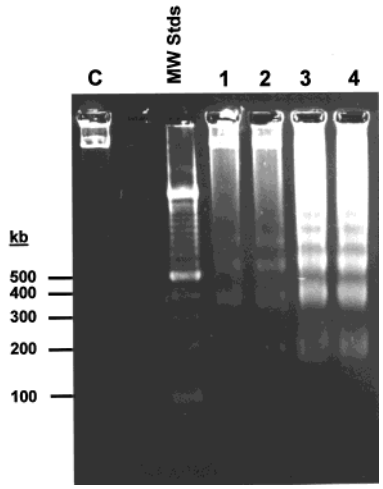

FIGURE 4: Internucleosomal DNA fragmentation following AMVN was not blocked by PAPANONOate. HL-60 cells were treated with 500 μM AMVN and/or 10 μM PAPANONOate for 4 h in serum-free RPMI. DNA was extracted from 1×10^6 cells and electrophoresed in a 2% agarose gel. Lane 1 represents control untreated cells, lane 2 represents cells treated with 10 μM PAPANONOate alone, lane 3 represents cells treated with 500 μM AMVN alone, and lane 4 represents cells treated with both PAPANONOate and AMVN. Lane C shows DNA obtained from untreated cells taken directly from stock cultures without any experimental manipulation. MW standards are shown for reference. The formation of DNA cleavage products corresponding to 180−200 bp ladders was clearly observed after AMVN alone and was unchanged by the simultaneous inclusion of PAPANONOate.

(B) DNA Fragmentation. Analysis of DNA fragmentation, another hallmark of apoptosis, was conducted to assess the potential of NO protection. Figure 4 shows the formation of DNA ladders characteristic of internucleosomal DNA cleavage following AMVN treatment. Control cells taken immediately from cultured stocks (C) showed essentially no 180−200 bp DNA "laddering". Control cells incubated for 2 h without addition of AMVN or PAPANONOate (lane 1) showed only traces of DNA fragmentation as did cells treated with PAPANONOate alone (lane 2), and this probably reflects the low basal amount of apoptosis observed under these conditions. On the other hand, treatment of cells for 4 h with AMVN alone produced marked DNA degradation in parallel to apoptotic nuclear morphology (see Figure 4). Inclusion of PAPANONOate with AMVN failed to eliminate internucleosomal DNA fragmentation.

Table 3: Caspase-3 Activation following AMVN Is Not Inhibited by PAPANONOate[a]

treatment	[PAPANONOate] (μM)	caspase-3 act. (nmol of product/1 $\times$ 10^6 cells) plus DTT	minus DTT
control	0	0.33 $\pm$ 0.01	0.03 $\pm$ 0.05
AMVN	0	2.38 $\pm$ 0.06	1.16 $\pm$ 0.09
AMVN	10	2.66 $\pm$ 0.11	1.02 $\pm$ 0.21
AMVN	50	2.66 $\pm$ 0.09	1.01 $\pm$ 0.10
AMVN	100	2.74 $\pm$ 0.02	1.09 $\pm$ 0.14
AMVN	500	2.86 $\pm$ 0.03	0.70 $\pm$ 0.13

[a] Data represent mean $\pm$ SEM of 3 observations.

(C) Caspase Activation. We next measured the ability of AMVN to induce caspase-3 activity in HL-60 cells in the presence of various concentrations of NO donor. Optimum analysis of caspase enzymatic activity requires DTT during the assay. Since DTT can potentially reverse nitrosylation of caspase-3, enzyme activity was measured in the presence and absence of this reducing agent. Table 3 shows the caspase-3 activity present in lysates of HL-60 cells treated for 2 h with 500 μM AMVN with or without various concentrations of PAPANONOate. In keeping with the apoptotic effects of AMVN observed above, caspase-3 activity measured in the presence of DTT was approximately 7-fold higher following AMVN relative to untreated control cells. Caspase-3 activity measured in AMVN-treated cells in the absence of DTT was reduced approximately 50% but was still substantially higher than that observed in untreated cells. The inclusion of 10 μM PAPANONOate, a concentration that produced maximal lipoprotective effects, had no effect on the ability of AMVN to induce caspase-3 activity. Increasing NO donor concentrations up to 500 μM, similarly, had no effect on AMVN-induced caspase-3 activation independent of whether DTT was present during the assay or not.

AMVN, NO, and PS Externalization and Translocation. Because of the membrane localization of PS externalization during apoptosis, phospholipid translocation poses a unique target for modulation by lipid peroxidation and lipoprotective antioxidants. We, therefore, next addressed the ability of NO to specifically modulate PS translocation during AMVN-induced apoptosis. We measured the extent of PS externalization following AMVN treatment in the absence and presence of lipoprotective concentrations of PAPANONOate using annexin V fluorescent flow cytometry. Figure 5 shows the percentage of annexin V positive/propidium iodide negative cells following 2 and 4 h AMVN treatment with and without PAPANONOate. In a manner analogous to that seen with the other measures of apoptosis, AMVN induced significant PS externalization, and the inclusion of the NO donor failed to ameliorate this effect.

The use of annexin V describes only the percentage of cells that have externalized PS but provides no quantitative information regarding the amount of PS externalized. Furthermore, annexin V provides no information regarding the externalization of the other major aminophospholipid, PEA. Therefore, we also labeled externalized PS and PEA using fluorescamine, a cell-impermeable fluorescent reagent capable of reacting with primary amines (*2*, *36*). Figure 6 shows the percentage of PEA (panel A) and PS (panel B) that was

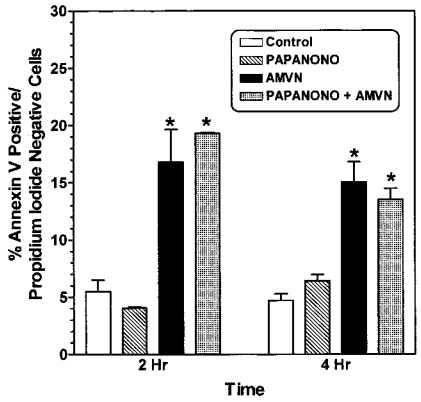

FIGURE 5: Annexin V binding to HL-60 cells treated with AMVN in the presence and absence of PAPANONOate. HL-60 cells were incubated in serum-free RPMI with or without 500 μM AMVN or 10 μM PAPANONOate as indicated at 37 °C. At the indicated times, cells were assessed for annexin V binding by flow cytometry as described under Materials and Methods. Data represent the mean $\pm$ SEM of the percentage of annexin V positive/propidium iodide negative cells obtained from three observations at each point. The asterisks denote a significant difference from control by one-way ANOVA and Neuman−Keuls multiple comparisons test.

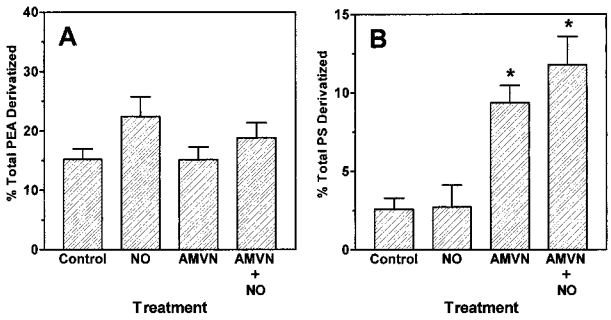

FIGURE 6: Comparison of PS and PEA accessibility to fluorescamine following AMVN and PAPANONOate treatment of HL-60 cells. Cells were treated with 500 μM AMVN and/or 10 μM PAPANONOate for 2 h in L1210 buffer and then reacted with fluorescamine as described under Materials and Methods. The percentage of total PS and PEA modified by fluorescamine was determined by phosphorus analysis of each modified phospholipid spot following two-dimensional HP-TLC and expressed relative to the amount of both modified and unmodified PS or PEA. Data represent the mean $\pm$ SEM for 4 samples per group. The asterisks denote statistically significant difference ($p < 0.002$) compared to untreated cells alone by Student's *t*-test.

modified by fluorescamine after a 2 h treatment of AMVN (500 μM) in the absence and presence of PAPANONOate (10 μM). Less than 3% of the total PS was available for fluorescamine derivatization in control untreated cells. AMVN produced a 4-fold increase in available PS (Figure 6B), which was essentially unchanged by the simultaneous treatment with NO donor. PAPANONOate alone did not increase the availability of PS to fluorescamine. The amount of PEA available on control cells was greater than that compared to PS (15%), and no significant changes were observed after AMVN or PAPANONOate (Figure 6A).

We next investigated how intramembrane oxidative stress may affect one particular enzyme function participating in these reactions, namely, aminophospholipid translocase (APT). APT normally serves a surveillance function that rapidly and efficiently internalizes any PS that appears in the external plasma membrane leaflet. The accumulation of externalized PS observed in our studies during AMVN

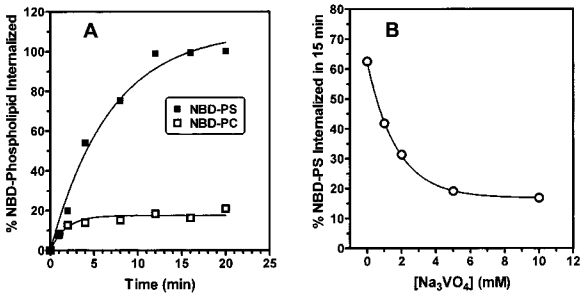

FIGURE 7: Characterization of aminophospholipid translocase activity in HL-60 cells. NBD-labeled PS and PC were incorporated into the external leaflet of the plasma membrane of HL-60 cells, and then internalization to a dithionite-resistant compartment was monitored over time as described under Materials and Methods. Panel A shows the time course and extent of internalization for both NBD-PS and NBD-PC. Panel B shows the extent of inhibition of NBD-PS internalization produced in the presence of various concentrations of Na_2VO_4.

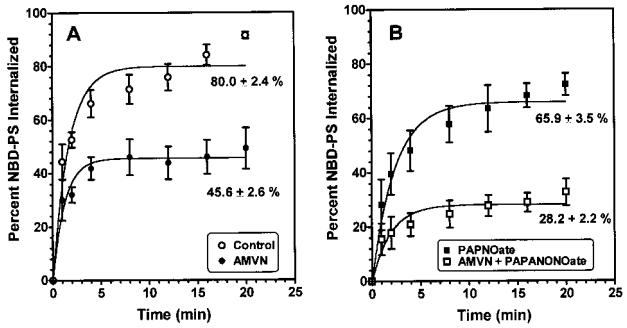

FIGURE 8: Effect of AMVN and PAPANONOate of aminophospholipid translocase activity in HL-60 cells. HL-60 cells were treated with 500 μM AMVN and 100 μM PAPANONOate in L1210 buffer at 37 °C for 2 h. Cells were then loaded with NBD-PS and processed for measurement of internalization as described under Materials and Methods. Data represent means ± SEM obtained for 7 experiments for control and 4 experiments for all other treatments. Curves were drawn by the fitting of the cumulative data set from each treatment to a one-phase exponential association model using GraphPad Prism Software. Maximal NBD-PS internalization expressed as percent of total available is shown for reference.

apoptosis clearly supports the idea that APT function is inhibited following AMVN treatment.

To measure APT function following the potential oxidant and antioxidant interactions arising during AMVN and PAPANONOate treatment, we utilized the fluorescent phospholipid substrates NBD-PS and NBD-PC. These labeled phospholipids were incorporated into the outer plasma membrane leaflet, and their internalization by APT to a dithionite-resistant location (internal membrane leaflet) was monitored over time. Figure 7A compares the ability of HL-60 cells to internalize NBD-PS and NBD-PC over time. NBD-PS was internalized at a rapid rate ($t_{1/2}$ for internalization about 4−5 min), and nearly all of the NBD-PS fluorescence became dithionite-resistant by 12 min. In contrast, almost all NBD-PC (approximately 80%) remained on the external surface over the 20 min incubation period, indicating that internalization was specific for aminophospholipids. The sensitivity of NBD-PS translocation to vanadate is shown in Figure 7B. Inclusion of Na_3VO_4 produced concentration-dependent inhibition of NBD-PS internalization as has been described by others (*37*) for this ATP-dependent enzyme activity. Thus, the activity of APT in intact HL-60 cells can be specifically characterized and measured by assessing the rate and extent of NBD-PS internalization.

Figure 8 compares the rates and extent of NBD-PS uptake in HL-60 cells treated with AMVN and/or PAPANONOate. Panel A indicates that treatment of HL-60 cells with AMVN for 2 h reduced the ability to HL-60 cells to internalize NBD-PS by approximately 2-fold (80% internalized in control vs 45% in AMVN-treated cells). The extent of sequestration also appeared to be partially inhibited after incubation of cells with the NO donor, PAPANONOate, alone (panel B, approximately 65% NBD-PS internalized). Moreover, the combination of PAPANONOate plus AMVN produced greater inhibition of NBD-PS translocation than observed with either agent alone and approximated only 30% of the total available for internalization.

AMVN, NO, and Oxidation of Thiols. Since AMVN-induced apoptosis occurred despite complete protection of membrane phospholipids, damage to other cellular targets must be critical to apoptosis. Because inhibition of the redox-sensitive APT was clearly resistant to the protective effects of NO and NO itself appears to have a detrimental effect on APT activity, it is possible that protein oxidation may be one locus for NO-resistant AMVN oxidative stress and subsequent apoptosis. Therefore, we next addressed whether AMVN could target other redox-sensitive moieties within the cell such as protein and nonprotein thiols. We employed the fluorescent maleimide-based reagent ThioGlo-1 to quantify reduced glutathione (GSH), the major small molecular weight sulfhydryl molecule in cells, as well as total protein SH groups. The GSH pool of thiols was first measured in the absence of SDS. SDS was added after initial titration was complete in order to expose protein sulfhydryls to the maleimide-based reagent. The initial thiol pool measured in the absence of SDS represents primarily GSH, although we cannot rule out that it may contain a small amount of other small molecular weight thiols and proteins with readily available hypersensitive sulfhydryl groups.

Table 4 shows the amount of SDS-independent (primarily GSH) and SDS-dependent (protein thiols) thiols measured after treatment of cells with 10 μM PAPANONOate and 500 μM AMVN alone or in combination. We first measured the GSH and protein thiol pools in crude cell homogenates without any subcellular fractionation. In addition, we repeated these analyses on a cytosolic-enriched supernatant that was obtained following a 10000*g* centrifugation. We observed that AMVN alone decreased the amount of GSH in the total homogenate by about 10% compared to untreated cells. A similar decrement in reduced GSH content after AMVN was observed in the cytosolic fraction as well. We also observed that AMVN induced similar changes in the protein thiol content when measured in the total cell homogenate. When protein thiols were measured in the cytosolic fraction after centrifugation, however, the content of protein thiols was unchanged by AMVN. This result implies that a pool of protein sulfhydryls contained within the membranes collected after centrifugation was oxidized by AMVN and was lost to measurement following centrifugation. Attempts to measure the total thiol content within the membrane fraction were compromised by a relative lack of sensitivity using this

Table 4: PAPANONOate Does Not Prevent AMVN-Induced Thiol Oxidation[a]

	GSH(−SDS) (nmol/10^6 cells)		protein thiols(+SDS) (nmol/10^6 cells)	
treatment	total lysate	cytosolic fraction	total lysate	cytosolic fraction
control	4.37 ± 0.08	4.12 ± 0.06	5.27 ± 0.08	3.73 ± 0.25
PAPANONO (500 μM)	4.59 ± 0.18	4.27 ± 0.16	5.32 ± 0.17	3.58 ± 0.28
AMVN (10 μM)	3.88 ± 0.08[b,c]	3.59 ± 0.07[b,c]	4.73 ± 0.10[b,c]	3.23 ± 0.09
PAPANONO + AMVN	4.09 ± 0.05[c]	3.80 ± 0.08[b,c]	4.75 ± 0.07[b,c]	3.52 ± 0.26

[a] Data represent mean ± SEM of 5−6 observations/point. [b] Denotes significant difference vs control ($p < 0.5$) based on one-way ANOVA and Newman−Keuls multiple comparison test. [c] Denotes significant difference vs PAPANONO alone ($p < 0.5$) based on one-way ANOVA and Newman−Keuls multiple comparison test.

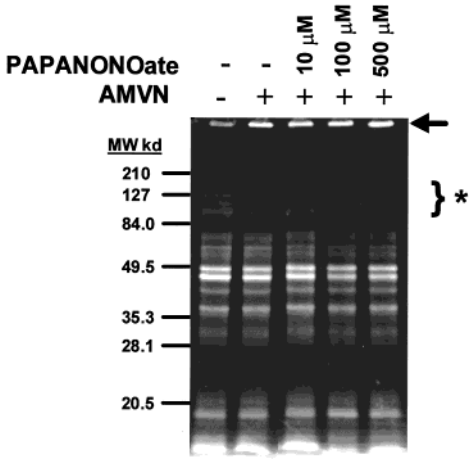

FIGURE 9: Electrophoretic separation of thiol-containing proteins in HL-60 cells treated with AMVN and PAPANONOate. HL-60 cells were treated with 500 μM AMVN and PAPANONOate as indicated for 2 h in serum-free RPMI at 37 °C. Cells were then recovered by centrifugation and protein extracts prepared as described under Materials and Methods. Proteins were labeled with ThioGlo-1; equivalent amounts of protein were loaded in each lane and run on an 8% acrylamide gel. Labeled proteins were then visualized under UV illumination (excitation 260−365 nm, 530 nm broad range emission filter). The locations of prestained standards (Bio-Rad) are shown for reference. The arrow indicates the accumulation of high molecular weight protein aggregates observed in the presence of AMVN regardless of PAPANONO treatment. The asterisk denotes the region where thiol proteins appeared selectively lost during AMVN and PAPANONO exposure.

method to measure the small thiol pool present in this fraction.

In contrast to its effects on AMVN-induced lipid peroxidation, PAPANONOate was ineffective at preserving the number of reduced thiols (both GSH and protein thiols) following AMVN. The amounts of protein thiols in the unfractionated lysate and GSH in the soluble fraction after treatment with both AMVN and PAPANONOate were significantly reduced as compared to both untreated and PAPANONOate-alone controls. While GSH in the unfractionated lysate measured after AMVN plus PAPANONOate was not statistically different from untreated controls, it was significantly different from PAPANONate alone. PAPANONOate treatment alone did not produce any appreciable change in the total number of ThioGlo 1 titratable sulfhydryls as measured in these crude cell fractions.

Analysis of thiol-containing proteins by SDS−PAGE also revealed small, but detectable oxidation of specific proteins following various NO/AMVN combinations. Figure 9 shows a representative SDS−PAGE separation of total cellular proteins from HL-60 cells stained with the fluorescent ThioGlo 1 reagent. The first lane shows the thiol staining profile of proteins obtained from control untreated cells. Little change in the overall thiol profile of most proteins was detected following AMVN. Significant accumulation, however, of ThioGlo-1 labeled proteins was observed at the top of the resolving gel (arrow) and probably represents oxidative aggregation and cross-linking of proteins. Protein aggregation was still observed when the lipoprotective concentration of PAPANONOate (10 μM) was included with AMVN treatment. Furthermore, AMVN-induced aggregation appeared to coincide with the loss of thiol-containing proteins from other regions within the gel, particularly in the region between 90 and 125 kDa. The loss of fluorescent labeling within various proteins on the gels was particularly evident after treatment with AMVN and higher concentrations of PAPANONOate (100 and 500 μM) and appeared greater than that observed with AMVN alone. PAPANONate alone at these concentrations produced labeling patterns essentially identical to unteated control cells (data not shown). Thus, NO does not appear to protect proteins from oxidation following AMVN in the same way that it protects phospholipids. In fact, high concentrations of NO may potentiate AMVN-induced loss of thiols at high concentrations.

DISCUSSION

Lipoprotective Effects of NO after AMVN. Debate has long raged over the prooxidant and antioxidant effects of NO (*7*). By virtue of its free radical nature, NO can participate in a variety of reactions that serve either to give rise to more reactive oxidizing species or to quench the steady-state concentration of various free radicals and prevent their interaction with other cellular substrates. For example, the reaction of superoxide and NO gives rise to the potent oxidant peroxynitrite (*38*). Peroxynitrite can induce specific protein oxidation at tyrosine residues (*39*), as well as oxidize protein and nonprotein sulfhydryls (*13*). On the other hand, NO can bind to redox-active metal centers and render then incapable of redox cycling, thus inhibiting metal-catalyzed lipid peroxidation (*40*).

In our studies, we initiated lipid peroxidation using the metal-independent generation of peroxyl radicals with AMVN. Thus, inhibition of metal-centered redox cycling is an unlikely mechanism to explain the lipoprotective effects of NO observed here. NO has recently been shown to inhibit lipoxygenase-induced lipid peroxidation of plasma lipoproteins (*41*) and superoxide/peroxynitrite-mediated oxidation of liposomes (*18*) through chain-terminating reactions with lipid peroxyl radicals analogous to vitamin E. NO rapidly reacts with organic peroxyl radicals at near diffusion-limited rates (*42*).

The consumption of NO during AMVN-induced lipid peroxidation, as detected with DAF-2DA, suggests that the

primary role of NO in our system is to react with radicals arising during AMVN decomposition or lipid peroxidation. We cannot, at present, determine if NO reacted directly with AMVN peroxyl radicals or with lipid-derived chain-propagating radicals (lipid peroxyl or alkoxyl radicals). Rubbo et al. have observed the formation of novel nitrogen-containing oxidized lipid products, indicating the possibility of the latter reaction (*18*). Nonetheless, NO must act early in the process since nearly complete inhibition of lipid peroxidation was observed. Using the rate constant ($R_i = 1.36 \times 10^{-6}$ mol L^{-1} s^{-1}) for the decomposition of azo-initiators described by Niki (*43*), we estimated that approximately 4.8 nmol/10^6 cells of peroxyl radicals was formed within 2 h exposure to 500 μM AMVN. This corresponds approximately to the amount of NO consumed (4.25 nmol/10^6 cells, 10 μM PAPANONOate) by AMVN-dependent processes at this time. Thus, there is a good agreement between the total amount of AMVN-derived radicals within the membrane and the amount of NO consumed.

O'Donnell et al. have postulated that the stoichiometry of the NO−peroxyl radical interaction is 2:1 according to the following reactions where LOO· and LO· are lipid peroxyl and alkoxyl radicals, respectively (*44*):

$$\text{LOO}\cdot + \text{NO}\cdot \rightarrow \text{LOONO} \rightarrow \text{LO}\cdot + \text{NO}_2\cdot$$

$$\text{LO}\cdot + \text{NO}\cdot \rightarrow \text{LONO}$$

One molecule of NO is consumed in the reaction with LOO·; however, the product LOONO is relatively unstable and probably decomposes to LO· and nitrogen dioxide radical. An additional molecule of NO is then required to react with and inactivate the lipid alkoxyl radical product. Hence, NO must be an extremely efficient lipoprotective antioxidant to achieve the complete protection of phospholipids observed in our studies.

PS Externalization and Aminophospholipid Translocase. A hallmark of apoptosis is the translocation of PS from the inner leaflet of the plasma membrane to the outer surface (*45, 46*) where it serves an important function for the recognition and engulfment of apoptotic cells by professional phagocytes prior to cell lysis (*3*). Aminophospholipid translocase is a membrane-bound ATP-dependent enzyme activity whose normal role is to transport aminophospholipids, PS and PEA, from the external to the internal leaflet of the plasma membrane (*4, 5*). Inactivation of this surveillance function of APT is, therefore, necessary to allow accumulation of PS on the exterior cell surface.

We have previously shown that selective oxidation of PS was an early event during the oxidant-induced apoptosis, preceded PS externalization, and was inhibited by overexpression of the anti-apoptotic gene, *bcl-2* (*1, 2*). These observations have led us to speculate that selective oxidation of PS occurred by an apoptosis-dependent mechanism different from random lipid peroxidation arising from oxidative stress. This notion was strengthened by our observation that PS oxidation was resistant to the vitamin E analogue 6-hydroxy-2,2,5,7,8-pentamethylchromane (*2*). Here we show that NO was able to inhibit PS oxidation during AMVN-induced apoptosis. Analysis of concentration−response relationships for PAPANONOate inhibition, however, revealed that more NO was required to protect PS than PC, PEA, and PI, which suggests that at least some of the PS oxidation occurred by a molecular mechanism distinct from other phospholipids. This mechanism is currently a focus of study in our laboratory.

Based on our earlier studies, we hypothesized that PS oxidation contributed to loss of APT function and was a prerequisite for PS externalization. One possibility is that oxidized PS is not effectively recognized by APT and, hence, remains on the cell surface once externalized. Second, modification of the APT protein during its interaction with a reactive PS oxidation product could result in loss of transport function. APT activity has previously been shown to be sensitive to oxidation and thiol modification (*47*−*49*). Here, we show, for the first time, that APT is inactivated following AMVN-induced membrane oxidation. Our data show that PS oxidation alone is not required for APT inactivation since NO plus AMVN inhibited APT to an even greater extent than AMVN alone, even when PS oxidation was inhibited. APT, however, may be similarly vulnerable to attack through NO-dependent nitrosation/oxidation reactions.

A number of proteins containing thiols critical for function have been shown to be inhibited following exposure to NO including Na^+/K^+-ATPase (*11*), metallothionein (*9*), and glyceraldehyde-3-phosphate dehydrogenase (*10*). NO probably does not directly react with free SH groups, but instead through, as yet undefined, reactions with its oxidation products such as nitrogen dioxide or peroxynitrite (*38*). While we did not observe a decrement in thiol content following exposure to PAPANONOate, we did observe a significant decrease in APT activity following the NO donor alone. This suggests that APT contains a SH group(s) critical for function that is (are) hypersensitive to NO or its oxidation products formed even in the absence of AMVN. Furthermore, NO potentiated the decrease in APT activity following AMVN exposure at a time when the formation of reactive nitrogen species, such as NO_2, would be favored as a consequence of the lipoprotective effects of NO described above. Since NO is relatively lipid-soluble (*n*-octanol/water partition coefficient = 6−8) (*7*), hypersensitive thiols on membrane proteins such as APT may be especially vulnerable to the nitrosating effects of NO.

Protein Thiol Oxidation/Nitrosation. We observed that protein and nonprotein thiols were oxidized following AMVN treatment. The major thiol measured in the absence of SDS is GSH. Depletion of GSH could represent its interaction with a limited number of AMVN- or lipid-derived radicals that may escape the membrane compartment or are processed by GSH and glutathione peroxidase directly or after their removal from the membrane by phospholipase.

In addition, we have observed a similar small, but significant, oxidation of protein thiols following AMVN when measured in total cell homogenates. Interestingly, this pool of sensitive protein thiols appears localized within the membranous fraction of the cell since a difference was not observed in the soluble fraction after centrifugation to remove the particulate fraction. The formation of high molecular weight protein aggregates observed here likely represents the formation of intermolecular cross-links and disulfide bridges as has been observed in mitochondiral proteins during oxidative stress-induced permeability transition (*50*). The fact

that protein aggregation was still observed without significant oxidation of *cis*-PnA suggests that protein cross-linking was not mediated by bifunctional aldehydic end products of lipid peroxidation such as malondialdehyde. Thus, certain thiol-containing proteins within the membrane may serve as targets for radicals derived during AMVN-dependent oxidations. Notably, these AMVN oxidations were insensitive to PAPANONOate treatment. Thus, the oxidative processes responsible for protein thiol oxidations following AMVN must be relatively insensitive to NO.

Alternatively, NO, or its products, may be capable of reacting with certain protein sulfhydryls that represent more sensitive targets for oxidation compared to membrane phospholipids. NO itself can catalyze the oxidation of SH groups to disulfides, but this process is relatively slow (*51*). NO cannot directly nitrosate SH groups, although one or more species produced during its autoxidation in aerobic solutions can (*38*, *51*, *52*). The identity of these species remains elusive but may include nitrogen dioxide (NO_2), dinitrogen trioxide (N_2O_3), and nitrosonium ion (NO^+). We should note that one of these, NO_2, is also formed during the reaction of NO with oxidized lipids (see above) and may explain the greater inhibition of APT observed with the combination of AMVN and PAPANONOate. The notion that protein thiols are direct targets for NO-dependent reactions is supported by the observation that depletion of thiol-containing proteins measured following SDS−PAGE was enhanced by the combination of AMVN and high concentrations of NO donor. In addition, NO alone appeared capable of inhibiting membrane-bound APT activity.

Thus, the lipoprotective effects of NO are not entirely sufficient to protect cells from AMVN-induced oxidative stress and subsequent apoptosis. We speculate that oxidation of specific proteins, especially within the membrane compartment of cells, is sufficient to signal the initiation of apoptosis following oxidative stress within this compartment. A number of regulatory proteins whose activity is modulated by redox mechanisms, presumably at hypersensitive thiols, include p53 (*53*), Ca^{2+}-ATPase (*54*), NF-κB (*55*), and heat shock proteins (hsp33) (*56*). The role of these or other proteins as targets responsible for any of the effects observed here remains a matter of speculation at the present time. It is noteworthy that the molecular mass of APT (115 kDa) (*57*) is included in the range of thiol-containing proteins (90−127 kDa, Figure 8) that are selectively decreased with AMVN and PAPANONO treatment. Therefore, the antioxidant effects of NO appear to be selective for the protection of lipids from oxidation, perhaps in accordance with its relative lipophilicity. Oxidative stress, however, is rarely restricted to a single compartment or molecular target. In this regard, we found that NO could not similarly protect proteins from oxidation, and, in fact, may itself disrupt protein function by direct modification.

Several workers have reported that NO can inhibit apoptosis, in part through thiol-mediated inactivation of caspases (*25*, *26*). The failure of NO to suppress apoptosis in our studies suggests that this effect may depend on the cell type studied, the type and concentration of NO donor employed, and the stimulus used to induce apoptosis. We studied the concentration-dependent effect of PAPANONOate on caspase-3 activation following AMVN and found that concentrations well above that required to inhibit lipid peroxidation failed to prevent the ultimate processing of procaspase-3 to its active form. We did not measure apoptosis at PAPANONOate concentrations greater than 100 μM, and it is important to point out that we did not measure caspase activity directly in the presence of NO. We cannot rule out that caspase-3 was indeed nitrosylated and inhibited in the presence of 100−500 μM PAPANONOate, but was rapidly denitrosylated under the conditions of the caspase assay. Our data, however, clearly show that PAPANONOate (up to 500 μM) did not block the upstream events of apoptotic initiation ultimately leading to caspase activation. It is clear that apoptosis was still observed in the presence of the maximal lipoprotective effects of PAPANONOate.

In conclusion, it is undisputed that lipid peroxidation plays a key role in cytotoxicity following oxidative stress. We demonstrate here for the first time, however, that complete protection of lipids from oxidation did not prevent apoptosis following oxidative stress. We show that the marked lipoprotective effects of NO are insufficient to protect cells from apoptosis following membrane-based oxidative stress initiated by AMVN. Small, but significant, oxidation of endogenous thiols (GSH and protein thiols) was also observed following AMVN and was unresponsive to concurrent exposure of NO. Thus, thiol oxidation initiated by AMVN may be an important signal for apoptosis. Membrane proteins, such as APT, may represent a class of hypersensitive molecular targets for AMVN- and/or NO-mediated redox events.

ACKNOWLEDGMENT

We thank Alexis Styche for excellent technical assistance in the performance of the flow cytometry assays.

REFERENCES

1. Fabisiak, J. P., Kagan, V. E., Ritov, V. B., Johnson, D. E., and Lazo, J. S. (1997) *Am. J. Physiol. (Cell Physiol.) 272 (*41*)*, C675−C684.
2. Fabisiak, J. P., Tyurina, Y. Y., Tyurin, V. A., Lazo, J. S., and Kagan, V. E. (1998) *Biochemistry 37*, 13781−13790.
3. Fadok, V., Voelker, D. R., Campbell, P. A., Cohen, J. J., Bratton, D. L., and Henson, P. M. (1992) *J. Immunol. 148*, 2207−2216.
4. Verhoven, B., Schlegel, R. A., and Williamson, P. (1995) *J. Exp. Med. 182*, 1597−1601.
5. Bruckheimer, E. M., and Schroit, A. J. (1996) *J. Leukocyte Biol. 59*, 784−788.
6. Nathan, C. (1992) *FASEB J. 6*, 3051−3064.
7. Rubbo, H., Darley-Usmar, V., and Freeman, B. A. (1996) *Chem. Res. Toxicol. 9*, 809−820.
8. Jia, L., Bonaventura, C., Bonaventura, J., and Stamler, J. S. (1996) *Nature 380*, 221−226.
9. Misra, R. R., Hochadel, J. F., Smith, G. T., Cook, J. C., Walkes, M. P., and Wink, D. A. (1996) *Chem. Res. Toxicol. 9*, 326−332.
10. Mohr, S., Stamler, J. S., and Brune, B. (1994) *FEBS Lett. 348*, 223−227.
11. Sato, T., Kamata, Y., Irifune, M., and Nishikawa, T. (1997) *J. Neurochem. 68*, 1312−1318.
12. Huie, R. E., and Padmaja, S. (1993) *Free Radical Res. Commun. 18*, 195−199.
13. Radi, R., Beckman, J. S., Bush, K. M., and Freeman, B. A. (1991) *J. Biol. Chem. 266*, 4244−4250.
14. Radi, R., Beckman, J. S., Bush, K. M., and Freeman, B. A. (1991) *Arch. Biochem. Biophys. 288*, 481−487.
15. Mulligan, M. S., Warren, J. S., Smith, C. W., Anderson, D. C., Yeh, C. G., Rudolph, A. R., and Ward, P. A. (1992) *J. Immunol. 148*, 3086−3092.

16. Matheis, G., Sherman, M. P., Buckberg, G. D., Haybron, D. M., Young, H. H., and Ignarro, L. J. (1992) *Am. J. Physiol. 262*, H616−H620.
17. Goss, S. P., Hogg, N., and Kalyanaraman, B. (1995) *Chem. Res. Toxicol. 8*, 800−806.
18. Rubbo, H., Radi, R., Trujillo, M., Telleri, R., Kalyanaraman, B., Barnes, S., Kirk, M., and Freeman, B. A. (1994) *J. Biol. Chem. 269*, 26066−26075.
19. Gaboury, J., Woodman, R. C., Granger, D. N., Reinhardt, P., and Kubes, P. (1993) *Am J. Physiol. 265*, H862−H867.
20. Wink, D. A., Hanbauer, I., Krishna, M. C., DeGraff, W., Gamson, J., and Mitchell, J. B. (1993) *Proc. Natl. Acad. Sci. U.S.A. 90*, 9813−9817.
21. Messmer, U. K., Reed, J. C., and Brune, B. (1996) *J. Biol. Chem. 271*, 20192−20197.
22. Blanco, F. J., Oches, R. L., Schwarz, H., and Lotz, M. (1995) *Am. J. Pathol. 146*, 75−85.
23. Mannick, J. B., Asano, K., Izumi, K., Kieff, E., and Stamler, J. S. (1994) *Cell 79*, 1137−1146.
24. Matthys, P., Froyen, G., Verdot, L., Huang, S., Sobis, H., Van Damme, J., Vray, B., Aguet, M., and Billau, A. (1995) *J. Immunol. 155*, 3823−3829.
25. Dimmeler, S., Haendeler, J., Nehls, M., and Zeiher, A. M. (1997) *J. Exp. Med. 185*, 601−607.
26. Kim, Y. M., Talanian, R. V., and Billiar, T. R. (1997) *J. Biol. Chem. 272*, 31138−31148.
27. Ritov, V. B., Banni, S., Yalowich, J. C., Day, B. W., Claycamp, H. G., Corongiu, F. P., and Kagan, V. E. (1996) *Biochim. Biophys. Acta 1283*, 127−149.
28. Folch, J., Lees, M., and Sloane-Stanley, G. H. (1957) *J. Biol. Chem. 226*, 497−509.
29. Chalvardjian, A., and Rudnicki, E. (1970) *Anal. Biochem. 36*, 225−226.
30. Langmuir, M. E., Yang, J.-R., Lecompte, K. A., and Durand, R. E. (1996) in *Fluorescence microscopy and fluorescent probes* (Slavik, J., Ed.) pp 229−234, Plenum Press, New York.
31. Kagan, V. E., Yalowich, J. C., Borisenko, G. G., Tyurina, Y. Y., Tyurin, V. A., Thampatty, P., and Fabisiak, J. P. (1999) *Mol. Pharmacol. 56*, 494−506.
32. Bottcher, C. J. F., Van Gent, C. M., and Pries, C. (1961) *Anal. Chim. Acta 24*, 203−204.
33. McIntyre, J. C., and Sleight, R. G. (1991) *Biochemistry 30*, 11819−11827.
34. Williamson, P., Bevers, E. M., Smeets, E. F., Comfurius, P., Schlegel, R. A., and Zwaal, R. F. A. (1995) *Biochemistry 34*, 10448−10455.
35. Krainev, A. G., and Bigelow, D. J. (1996) *J. Chem. Soc., Perkin Trans. 2*, 747−754.
36. Rawyler, A., Roelofsen, B., and Op den Kamp, J. A. (1984) *Biochim. Biophys. Acta 769*, 330−336.
37. Williamson, P., Kulick, A., Zachowski, A., Schlegel, R. A., and Devaux, P. F. (1992) *Biochemistry 31*, 6355−6360.
38. Pryor, W. A., and Squadrito, G. L. (1995) *Am. J. Physiol.*, L699−L722.
39. Ischiropoulos, H., Zhu, L., Chen, J., Tsai, M., Martin, J. C., Smith, C. D., and Beckman, J. S. (1992) *Arch. Biochem. Biophys. 298*, 431−437.
40. Gorbunov, N., Osipov, A., Day, B., Zayas, B., Kagan, V. E., and Elsayed, N. (1995) *Biochemistry 34*, 6689−6699.
41. Rubbo, H., Parthasarthy, S., Kalynaraman, B., Barnes, S., Kirk, M., and Freeman, B. A. (1995) *Arch. Biochem. Biophys. 324*, 15−25.
42. Padmaja, S., and Huie, R. E. (1993) *Biochem. Biophys. Res. Commun. 195*, 539−544.
43. Niki, E. (1990) *Methods Enzymol. 186*, 100−108.
44. O'Donnell, V. B., Chumley, P. H., Hogg, N., Bloodsworth, A., Darley-Usmar, V. M., and Freeman, B. A. (1997) *Biochemistry 36*, 15216−15223.
45. Martin, S. J., Reutelingsperger, C. P. M., McGahon, A. J., Rader, J. A., van Schie, R. C. A. A., LaFace, D. M., and Green, D. R. (1995) *J. Exp. Med. 182*, 1545−1556.
46. Vermes, I., Haanen, C., Steffens-Nakken, H., and Reutelingsperger, C. A. (1995) *Immunol. Methods 184*, 39−51.
47. Herrmann, A., and Devaux, P. F. (1990) *Biochim. Biophys. Acta 1027*, 41−46.
48. Morrot, G., Herve, P., Zachowski, A., Fellman, P., and Devaux, P. F. (1989) *Biochemistry 28*, 3456−3462.
49. de Jong, K., Geldwerth, D., and Kuypers, F. A. (1997) *Biochemistry 36*, 6768−6776.
50. Bindoli, A., Callegaro, M. T., Barzon, E., Benetti, M., and Rigobello, M. P. (1997) *Arch. Bichem. Biophys. 342*, 22−28.
51. Pryor, W. A., Church, D. F., Govindan, C. K., and Crank, G. (1982) *J. Org. Chem. 47*, 156−159.
52. Wink, D. A., Nims, R. W., Darbyshire, J. F., Christodoulou, D., Hanbauer, I., Cox, G. W., Laval, F., Laval, J., Cook, J. A., Krishna, M. C., DeGraff, W. G., and Mitchell, J. B. (1994) *Chem. Res. Toxicol. 7*, 519−525.
53. Hainaut, P., and Milner, J. (1993) *Cancer Res. 53*, 4469−4473.
54. Liu, G., and Pessah, I. N. (1994) *J. Biol. Chem. 269*, 33028−33034.
55. Schreck, R., Albermann, K., and Baeuerle, P. A. (1992) *Free Radical Res. Commun. 17*, 221−237.
56. Jakob, U., Muse, W., Eser, M., and Bardwell, J. C. (1999) *Cell 96*, 341−352.
57. Tang, X., Halleck, M. S., Schlegel, R. A., and Williamson, P. (1996) *Science 272*, 1495−1497.

BI9912544